

TABLE III. Results of postshock anneal.

Anneal temperature (°C)	Time duration (min)	$\frac{R_{4.2}}{R_{298}}$
Preanneal	•••	0.0222
55-58	17	0.0232
94-97	10	0.0229
199-207	7	0.0064

tions from the cold-rolled foil; impurity clustering could also take place. Density of dislocations removed by anneal was calculated from liquid-helium-temperature resistance measurements on MRC foil before and after anneal. Using published dislocation resistivity in silver<sup>21</sup>

$$\Delta\rho = (1.9 \times 10^{-13} \mu\Omega \text{ cm}^3)\Lambda$$

( $\Lambda$  is dislocation line density), the result was  $2 \times 10^{10}$  cm/cm<sup>3</sup>. This dislocation density is within reason for cold-rolled metals;  $5 \times 10^{11}$ /cm<sup>2</sup> is quoted by Hull<sup>56</sup> for heavily cold-rolled metal.

Previous shock work shows a variety of effects of initial dislocation density on shock response. Work on single-crystal copper shows that 3.5% prestrain reduces the initial elastic stress jump after 5 mm of shock propagation to near zero; a ramping precursor wave then follows the jump.<sup>57</sup> (The prestraining increased dislocation density to  $10^9$  from  $10^6$ /cm<sup>2</sup>.) Shock hardening of annealed nickel, on the other hand, was independent of prestrain, prestrained by cold rolling to as much as 80% reduction in thickness.<sup>58</sup> Also, a change of an order of magnitude in initial dislocation density did not significantly affect precursor decay in lithium fluoride.<sup>50</sup>

From the standpoint of the jog model, one might expect greater initial forest dislocation density in unannealed foil to result in more jogs and hence more defects. This is one possible explanation of the trend of the data.

### I. Discussion of resistivity time dependence

It is possible that the resistance-time structure observed for  $\frac{1}{2}$   $\mu$ sec in the present experiments may result from deformation processes associated with stress relaxation and possibly point-defect rearrangement and annihilation. However, enough ambiguity exists among the records to discourage detailed conjecture on the physical meaning of the resistance-time structure.

### J. Work on recovered silver foil

Silver foils recovered after impact experiments were studied by observing resistance changes on annealing and by optical and scanning electron microscopy.

Pieces of silver foil up to 0.8 cm long and 0.25 cm wide were recovered in air in four shots; the shots were 73-009, 73-010, and 73-013 on MRC silver and 73-044 on W3N silver. The impact-target assembly, decelerated by nylon rags, was recovered with the silver and sapphire fragments trapped inside. Although the state of the recovered foils was affected by the relief and deceleration processes, it may give some clues to the nature of the shocked state.

A simple annealing study was made of the resistance of a foil piece recovered from shot 73-010 shocked to 87 kbar. The preshock value of the resistance ratio between liquid-helium temperature and room temperature was 0.00438. As recovered, two different foil pieces gave postshock values of 0.0222 and 0.220, five times larger than the preshock value. For shot 73-013 (27 kbar) the preshock value was 0.00376; the postshock value was 0.0178, 4.7 times as large.

The preshock resistance at 4.2°K should be due mainly to impurities. The difference between the postshock and preshock values should be due to lattice imperfections remaining after the shock process. For shot 73-010 the resistance-ratio difference is 0.0178; for 73-013, 0.0140.

A piece from 73-010 was annealed isothermally and postanneal resistance ratios were obtained; results are given in Table III. The table shows that annealing at less than 100°C caused almost no change in the imperfection resistance; if anything, the resistance increased slightly. (The same behavior was noted in shocked copper.<sup>59</sup>) Rearrangement or dispersal of imperfections could cause this. Annealing at 200°C does remove two-thirds of the shock-induced resistivity remaining after postshot recovery. A 50°C anneal should remove all isolated point defects created by plastic deformation.<sup>55</sup> Evidently any point defects generated by shock compression were able to annihilate, migrate to the surface, or cluster after relief to 1 atm in the impact experiment. The clusters, on the other hand, may be stable to higher temperatures.<sup>60</sup> In addition, the study of deformed silver by Bailey and Hirsch<sup>61</sup> indicated that dislocation density does not change until recrystallization after several hours at 208°C. Hence, the resistivity change in the 200°C anneal is probably due to annihilation of vacancy clusters. Using estimates by Martin and Paetsch for resistivity of clusters,<sup>38</sup> the vacancy concentration corresponding to the resistivity change due to the 200°C anneal is  $(0.2-0.8) \times 10^{-3}$ . This compares to an estimated vacancy concentration behind the shock wave of  $10^{-3}$  for that shot.

Examination of recovered foils under an optical microscope at magnifications of 30-100 showed sets of lines locally parallel which were not present in unshocked foil. These same lines were also observed by scanning electron microscopy (Fig. 10); similar lines have been observed in shocked nickel by Dieter.<sup>62</sup> Dieter identifies the lines as slip bands (clusters of closely spaced slip lines). In the present work, as in the nickel work the slip bands are fragmented due to cross slip. In neither case is there evidence of deformation twins.

Average slip-band spacing in the nickel work was  $2.7 \pm 0.3 \mu\text{m}$  for all shock strengths (100-520 kbar). For the present work  $1.4 \pm 0.5 \mu\text{m}$  was a typical mean value for the observed spacing of primary slip bands. Some evidence of slip on secondary planes was observed with a spacing of about  $8 \mu\text{m}$  [Fig. 10(b)]. Nickel shocked to 100 kbar showed no secondary slip, but at 460 kbar secondary slip was seen.

Dieter notes that the slip-band spacing in recovered

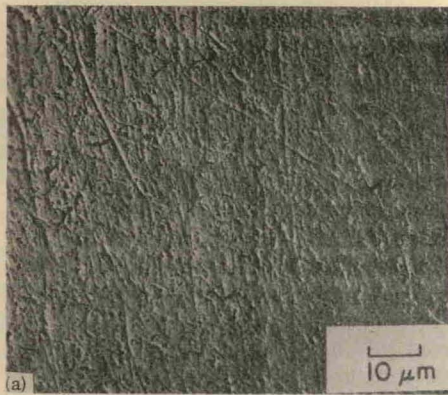


FIG. 10. Scanning electron micrographs of shocked and unshocked silver foil. (a) Unshocked MRC foil. (b) Recovered foil from shot 73-009. Note evidence of cross slip, secondary slip, and grain boundaries.

nickel may be representative only of the residual strain following shock compression and relief. The slip-band spacing observed corresponds roughly to that expected from slow deformation to the residual strain value. Similarly, observed slip-band spacing in silver is possibly typical of the final relieved state and not of the compressed state.

## V. CONCLUSIONS

Accurate and reproducible measurements of resistance changes in silver foils due to shock-wave compression were accomplished. These results were made possible by careful preparation of well-characterized specimens and by careful design of the impact experiment. Experimental accuracy was sufficient to resolve an effect of silver purity on the electrical resistance or resistivity as a function of shock pressure. A smaller effect of annealing prior to shock loading also appears to be discernible. The reproducibility of the structure of voltage-time profiles obtained during the  $\frac{1}{2}$   $\mu$ sec of shock compression was shown in one case and consistent trends in profile shape were demonstrated in a number of other cases. The structure of the voltage-time profiles appears to depend on purity and state of anneal of the foil and on pressure.

Vacancy concentrations as high as  $2 \times 10^{-3}$  per lattice site were estimated from the deviation between isothermal shock resistivity data and hydrostatic results. Annealing and microscopy studies on silver foils recovered after the shock experiments tended to confirm these concentrations as well as giving evidence for dislocation slip processes. The high vacancy concentrations may be evidence for dislocation speeds near shear-wave speed. Vacancy concentrations generated were found to vary as the three-halves power of the total strain.

Calculations involved in analyzing data have themselves provided some interesting results. An approximate semiempirical calculation of resistivity vs hydrostatic pressure has been established and used to extrapolate existing experimental data beyond 30 kbar. Such calculations should prove useful in other high-pressure work.

## ACKNOWLEDGMENTS

The authors are indebted to G.E. Duvall and D. Lazarus for helpful discussions. The help of P. Bellamy in operating the high-velocity impact facility and J. Guptill for technical support work is gratefully acknowledged. The work of J.J. Dick was supported by a National Defense Education Act Fellowship and the U.S. Air Force Office of Scientific Research under Contract No. 71-2037.

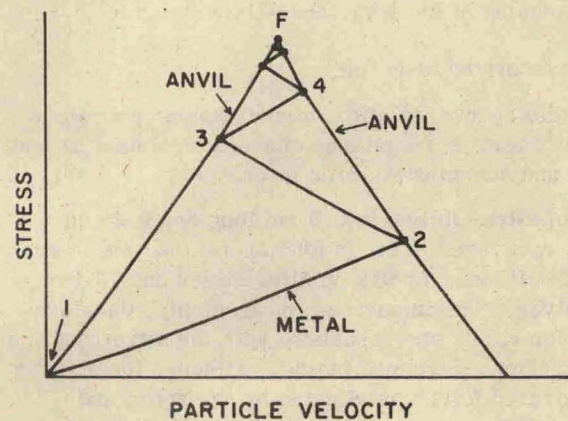
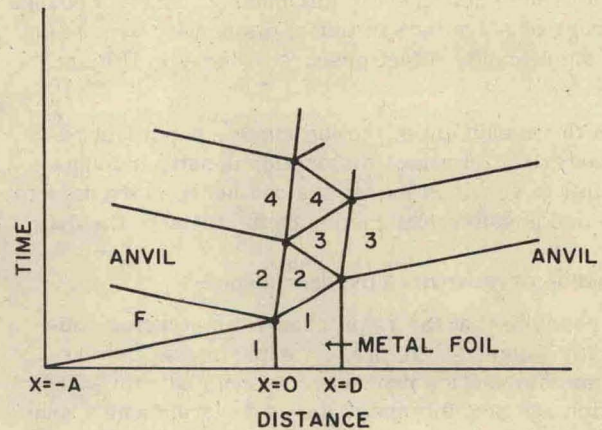


FIG. 11. Reverberation states in  $(t, x)$  and  $(P_x, u)$  planes.